

Laser speckle metrology – a tool serving the conservation of cultural heritage

K. D. Hinsch

Applied Optics, Institute of Physics, Carl von Ossietzky University Oldenburg
26111 Oldenburg, Germany

Abstract. Deterioration of artwork is often connected to mechanical material degradation that starts at microscopic scales. Insight into decay mechanisms can therefore be obtained by monitoring microscopic deformation and displacement fields. Thus, the proper optical methods become an ideal tool for restorers and conservators, the more as the methods are non-intrusive and remotely applicable. We show how the scope of modern speckle metrology can be adapted to this aim. Refinements of correlation imaging, speckle interferometry and low-coherence detection as well as the time average monitoring of vibrations provide a wealth of methods that have been applied successfully in historical objects.

1 Introduction

For many years the preservation of artwork was mainly the domain of the humanities. Lately, however, science is playing an increasing role in the analysis, conservation and restoration of historical objects. For unique and delicate specimens – from skilfully carved stone sculptures to colourful medieval wall paintings – analytical techniques must be non-invasive. Optics is providing a powerful and versatile set of tools for surveying and analyzing historical treasures [1–3]. Since they were made these priceless objects have aged. They deteriorate due to varying climate conditions or polluted environments and their preservation requires special countermeasures. Critical monitoring of the state of the object, identification and understanding of the deterioration processes and control of remedies are important.

Often, deterioration starts at the microscopic level, initially producing weakening of the mechanical cohesion in the sample. This shows up in irregular minute displacements or changes in the micro-topography of an objects surface. Thus, optical contouring and deformation mapping methods can provide essential data on the distribution of mechanical stress in the sample, indicate weak spots, or provide early-warning data on objects at risk. Suitable methods must provide sufficient sensitivity to detect displacements or changes in the topography well down in the micrometer domain. Yet, they should still operate successfully on-site in spite of disturbances like rigid-body creeping motions, annoying vibrations or air turbulence. The state of the object may also be checked by monitoring its deformation response to an external mechanical or thermal load (comparable to the medical checkup in health care).

Generally, any of the optical methods for displacement mapping that are employed in experimental mechanics are also suited for the present task – provided they are robust enough to be applied in an environment outside a laboratory. Optical techniques are often based on the evaluation of the laser light field scattered from the surface under inspection. This field is characterized by its random nature – manifest in the speckled appearance of the image of the object. This laser speckle pattern can be considered a “fingerprint” of the surface and its analysis may provide the wanted data on object changes. This may be done by correlation of the speckle intensity fields using comparatively simple equipment. The motion of the fingerprint, so to speak, provides displacement data at sensitivity well in the micrometer range. Thus, the delicate response of pieces of art to environmental loads or an artificial external stimulus can be monitored. At the same time any small change in the fingerprint pattern provides a measure for average changes in the surface profile that may quantify the deterioration attack on the surface. For the detection of still smaller displacements (sub-wavelength sensitivity) interferometric methods that measure phase shifts are needed.

The present article introduces characteristic features of speckle metrology and illustrates its basic performance in art monitoring. Then it concentrates on recent sophisticated refinements to extend the performance to specific situations at delicate objects or in unfavourable measurement environments that otherwise would rule out this kind of sensitive optical metrology. Finally, we devise novel approaches that explore the situation even underneath a surface.

2 Digital image correlation – displacement fields, surface deterioration and ablation monitoring

When a rough-surface object is viewed or photographed in laser-light illumination its image is covered with a granular pattern of speckles [4]. These are produced by interference of the many elementary light waves scattered from the irregularities of the surface. The random phases imposed on the light produce interference of statistically varying outcome. Thus the speckle pattern is taken as the fingerprint of the surface – encoded by the optical system doing the observation. Any displacement of the surface will produce an according motion of the speckle pattern and any changes in the microscopic topography of the surface will alter the speckle pattern.

To measure the displacement field of a sample surface we just need to take an image of the object before and after the motion – usually with an electronic camera. The images are then evaluated by determining locally the shifts of the recorded speckle patterns. For this purpose, the images are subdivided into a matrix of small interrogation regions. For each of the sub-images the displacement field is computed from a two-dimensional cross correlation – thus the technique is often termed Digital Speckle Correlation or Digital Image Correlation (DIC) [5]. The advantage over traditional techniques is that the surface need not show visual details nor do we have to affix any markings to the object. Furthermore, high sensitivity can be obtained by using small-sized speckles which is achieved by stopping down the imaging aperture. Sophisticated algorithms yield the displacement field with sub-pixel resolution

of roughly a micrometer. Mind, however, that the method is primarily limited to detect displacements normal to the viewing direction, the so-called in-plane component. The experimental setup is extremely simple consisting of light source, CCD-camera and computer.

Practically, the displacement value is obtained from the position of the cross-correlation peak. Successful performance of the method thus requires a certain similarity of the speckle patterns in both the images compared – otherwise correlation is lost and the peak degrades. When decorrelation of the speckle patterns becomes an issue during large displacements or significant changes in the surface a white-light version of image correlation may help. Provided there is sufficient image texture from details in the object the laser is replaced by a traditional light source and correlation is based on the motion of image details. The resolution in this case is set by the fineness of the image details.

DIC in either version is an established technique and has been applied repeatedly also to tasks in artwork diagnostics. For on-site investigations the white-light version provides a robust setup of sensitivity well in the μm -range. We used it, for example, in the monitoring of the response of antique leather tapestry to changes in temperature and humidity. Laser speckle instruments were used in the same project to determine basic data of leather under mechanical and thermal loads [6].

In its primary form, DIC gives only the in-plane displacement data. It was shown, however, that it can even provide a three-dimensional displacement vector. An analysis of the shape of the correlation peak or the cross power spectrum of the speckle images under comparison provides the local tilt from which the out-of-plane displacement can be calculated by integration [7]. The accuracy of the component thus obtained, however, falls one order of magnitude short of the in-plane component.

We mentioned that decorrelation is of disadvantage in displacement mapping. On the other hand, the reduction in the correlation coefficient can be used as a measure for changes in the topography of a rough surface. These could be evidence for micro-scale processes fuelling artwork deterioration. We have employed such decorrelation analysis for various issues in artwork research [8]. Typical situations are the monitoring of salt crystals growing on historical murals or an estimate of the impact of repeated water condensation on the historical substance in natural building stones. Let us show the typical performance by another example.

Lasers are often used to clean artwork by ablation of dirt. Efficient monitoring of the ablation process is needed to make sure that only the dirt is removed and no damage is done to the invaluable substance underneath. For this purpose we took speckle images of the surface under treatment for each laser shot and used the decrease in the correlation coefficient to indicate the amount of matter removed. A thorough analysis with varying surface models had to be carried out to quantify the relation between average change in the surface profile and decrease in correlation [8]. Fig. 1 presents a set of correlation coefficients versus the number of laser shots in the cleaning of a sandstone sample by green 400-mJ Nd:YAG-laser pulses. Our modelling allowed us to assign an average removal of 70 nm to a correlation coefficient of about 0.1. The family of graphs is obtained by taking every second image as a new reference image. The results show that the first pulse already removes about 70 nm; later pulses, however, produce decreasing effects. In suitable object/dirt combinations we

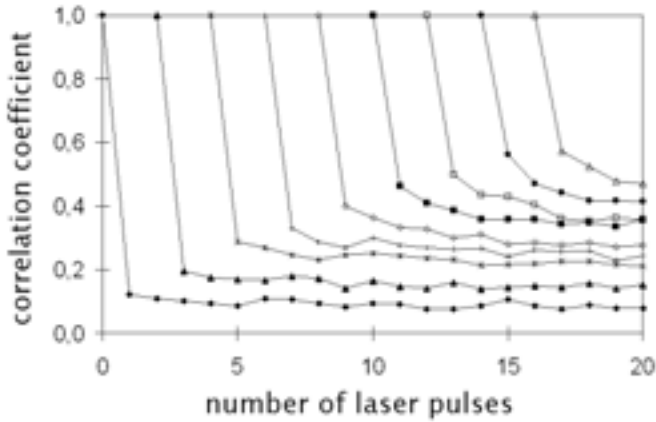


Figure 1. Monitoring of dirt removal from a historic sandstone sample by speckle correlation. Material is ablated by green Nd:YAG-laser pulses. The family of graphs is obtained by using new reference images in the course of the process.

expect that the rate of ablation will change markedly when the underlying substance is reached.

3 Video holography – mechanical response of historical murals to sunshine

Displacements well below a micron can be detected by interferometric methods. This is achieved by phase-sensitive recording of the speckle light with the aid of a reference wave in a setup for video-holography, mostly called Electronic Speckle Pattern Interferometry (ESPI) [9]. Here, too, the object under investigation is illuminated by laser light and imaged by a CCD-camera (Fig. 2). Now, however, a spherical reference wave is superimposed via a beamsplitter producing an interference image (image plane hologram) available for further processing in a computer. Subtraction of successive images, for example, yields a system of so-called correlation fringes. These are contour lines of constant displacement in the direction of a sensitivity vector \mathbf{k} that is determined by the difference in illumination and observation directions. For normal illumination and viewing, for example, \mathbf{k} points into the out-of-plane direction. In combining several optical setups of different geometry all three spatial components of a displacement vector can thus be determined. The interpretation of a single fringe system is ambiguous – it does not tell us the sign of the displacement. Furthermore, jumps in the fringes that occur when discontinuities in the displacement field are involved impede evaluation. To handle these problems several images need to be recorded for each of which the reference wave has undergone a set phase shift. Often three or four images at regular phase intervals are collected – a strategy

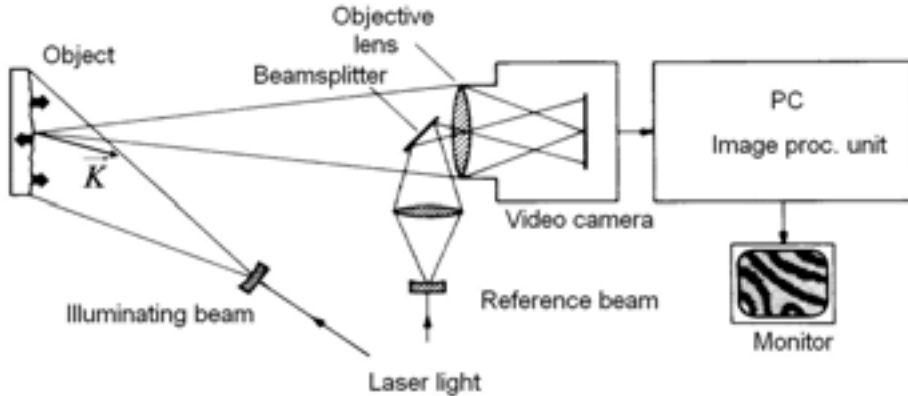


Figure 2. Optical setup for deformation measurement by video holography (Electronic Speckle Pattern Interferometry – ESPI).

known from classical interferometry as phase shifting. Such a series of images allows automated evaluation by a procedure called spatial phase unwrapping and provides unambiguous deformation data [10].

ESPI may also be used in the measurement of amplitudes in sinusoidal vibrations – a feature that we will use in the monitoring of loose plaster layers at murals. If we assume that the vibration period is short compared with the recording time the signal in the electronic camera is a time average over the interference signal at all phases. Proper electronic or digital processing of this signal produces fringes contouring the vibration amplitude.

To introduce the matter, outline the problems that need improvements, and illustrate the type of data obtained we show some early results from a project where traditional ESPI provided answers to urgent questions of the conservators. The work concerned the role of solar irradiation in the decay of 19th-century murals in Wartburg castle of Thuringia, Germany. This castle is the famous place where Martin Luther translated the bible into German around 1520. The legend says that he had to fend off the devil by throwing his inkpot at him! A conventional ESPI system was rigidly attached to the wall. It used laser-diode illumination and phase shifting by successive piezo-electrically driven tilt of a glass plate in the reference wave. The thermal load on the fresco was estimated by mapping deformations during cyclic heating and cooling – sunshine being simulated by infrared irradiation. In the left part of Fig. 3 we show the area of observation in the mural and at the right the deformation field produced during a 2.5-minute period in a cooling-off phase. A characteristic feature is a sudden kink in the displacement running through the field and coinciding with an image detail in the painting. Obviously, such an abrupt change will be accompanied by high local tensions in the material that will pose a threat to the integrity of the substance – a good reason to ban all direct sunlight from the frescos.

The coincidence of the location of the displacement irregularity with the feature line in the painting provided an interesting explanation for the discontinuity in the

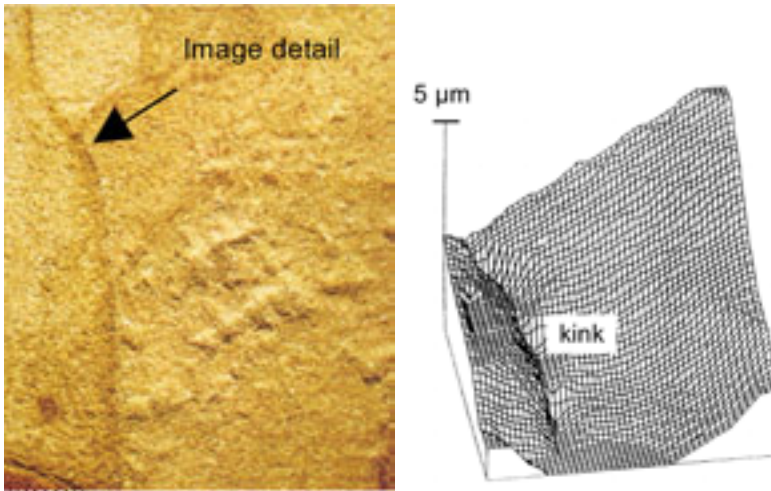


Figure 3. ESPI study of the thermal response of a fresco in Wartburg castle, Thuringia, Germany. Left: measuring field (width 6 cm); right: displacement map showing deformation kink at the location of a former boundary of work-piece.

mechanical response. Here, two work pieces meet that the painter has produced at different times. Frescos are painted onto fresh plaster and the artist scrapes off unused plaster when he finishes a days work. Our measurement result suggests that new plaster does not attach well to the old. The poor mechanical contact is a source for future problems. 150 years after the frescos were painted we uncovered where the artist made a break in his work – although he tried to hide it underneath the feature line in the image!

This example illustrates a typical implementation of optical metrology in the monitoring of artwork. Long-term changes in a specimen are difficult to register directly because this would require a stable measuring device at the object for a very long time. Rather, such changes are revealed in regular checkups by repeatedly exposing the specimen to a standard load and studying any changes in its response.

4 New challenges for ESPI (electronic speckle pattern interferometry)

Our continuing optical activities at cultural-heritage objects revealed that early-day ESPI needed substantial improvements to cope with the problems generally met in the practical study of artwork. The quality of the measurements suffered from spurious signal fluctuations during observation and data acquisition that originated from background vibrations, turbulence in the optical path or rigid-body misalignments. Sometimes, the technique was just too sensitive for the process encountered, sometimes the deformation rate was too rapid to obtain correct phase-shifted data; often the light source lacked coherence or was instable. Let us therefore turn towards more refined techniques that take up such shortcomings and provide some novel innovative approaches.

We have learned that a successful ESPI system requires provisions for phase shifting. For each state of the object several frames are needed that have been taken at a set of given phase differences between object and reference wave. The system used at the Wartburg employed temporal phase shifting (TPS) where the phase shifts are produced in succession by changing the optical path length in one optical branch. This can be imposed by turning a glass plate, translating a mirror or stressing a glass fibre in the optical delivery. Processing of the phase-shifted frames produces a phase map mod 2π which is displayed in a saw tooth grey-level or pseudo-colour representation.

During live observations of non-stationary objects like pieces of art in their everyday environment the conditions may change in time faster than allowed by the time-out required for phase shifting. Even if the object deformation is sufficiently slow, the measured phase is often deteriorated by air turbulences in the optical path or by background vibrations. Therefore, schemes have been developed to obtain the phase data simultaneously.

The most successful concept in which at least three phase-shifted images are recorded on the same CCD-target in the camera is called spatial phase shifting (SPS) [11,12]. For this purpose the source of the spherical reference wave originating in the aperture of the imaging optics (cf. Fig. 2) is given a small lateral offset resulting in a linear increase of the phase along one direction on the target. This offset must be adjusted such that the period of the carrier fringes resulting from interference of object and reference wave equals three times the pixel pitch in the offset direction. Then the reference-wave phase between adjacent pixels differs by 120° and the combination of data from three neighbouring pixels each gives the necessary phase-shifted frames. These can be combined in the commonly used phase-shifting algorithms to produce the mod 2π saw tooth pattern. For our purposes another evaluation method, the Fourier-transform technique [13], is more appropriate, because it offers additional features as we will see soon.

Let us briefly describe this technique which yields the complex-valued (amplitude and phase) light distribution in the image plane that can be utilized to calculate the phase difference data of subsequent images needed to determine the displacement. We mentioned the carrier fringes due to the superposition of object-light and off-axis reference wave. Fourier-transformation of the CCD-image thus yields a zero-order term and two side-band terms at the carrier frequency, both of which contain the complex spatial frequency spectrum of the object light. Careful matching of pixel data (size and pitch), speckle size and reference wave offset will guarantee non-overlapping spectral terms and maximum free spectral range. Thus, any one of the sideband terms can be separated for inverse Fourier-transformation to yield the complex object-light distribution and thus the wanted object-light phase.

Let us demonstrate the superiority of spatial (SPS) over temporal (TPS) phase shifting by observing a static deformation (point-like load at the centre of a membrane) that is disturbed by background vibration (insufficient vibration insulation of the setup) or hot turbulent air in the viewing path (Fig. 4). Obviously, TPS (upper frames in Fig. 4) results in poor-quality saw tooth images when vibrations cause wrong phase shifts and thus a loss of directional information (centre) or when small-scale turbulence creates even locally varying phase shifts so that the correct-

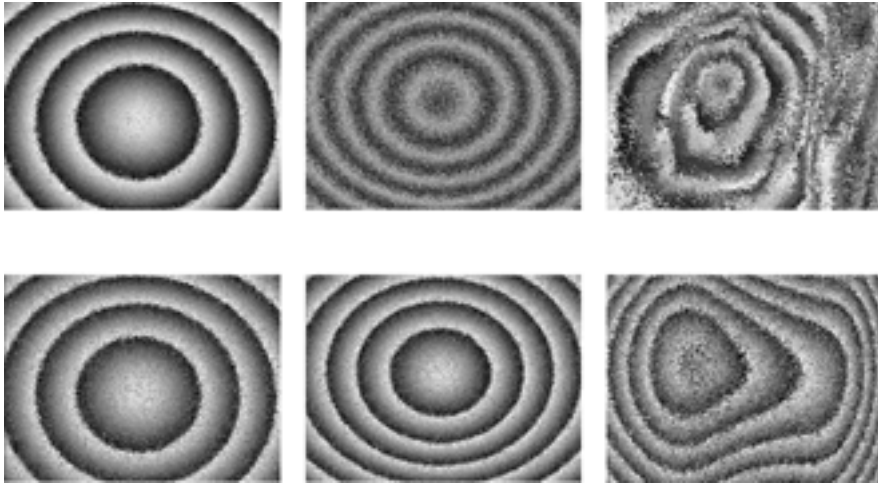


Figure 4. Deterioration of the saw tooth phase maps in an ESPI deformation study under stable experimental conditions (left) and disturbed by vibrations (centre) or air turbulence (right). Performance of temporal phase shifting TPS (upper) versus spatial phase shifting SPS (lower).

ness of the image is partly lost (right). Due to the greatly improved performance of SPS (lower frames – under the same conditions) we decided therefore to implement this arrangement whenever possible. Comparison of both the static images (left), however, illustrates that under stable conditions SPS performs slightly inferior due to residual fluctuating speckle phase over the three pixels compared [14].

For an overall displacement map characterizing the process under investigation the steps in the mod 2π -maps have to be eliminated – a procedure called spatial phase unwrapping. The usual way is to detect locations of the 2π jumps by comparing neighbouring phase values and converting the step function into a continuous displacement phase by adding the required integer multiples of 2π . This procedure is carried out along suitable tracks in the image – thus the name spatial phase unwrapping. In the history of ESPI, effective unwrapping algorithms that are resistant to a propagation of errors have been an important issue. They easily work in good-quality data fields. Real-world objects like those we are concerned with in this article, however, pose real challenges.

The problem can be nicely illustrated by the response of a piece of historic brick, 2 cm in thickness, to cyclic heating and cooling with an infrared radiator (Fig. 5). The white-light image of the specimen, Fig. 5 left, already implies some difficulties to expect. We see that a network of cracks divides the brick into numerous sub-areas that probably each will execute an independent deformation. Indeed, the out-of-plane displacement phase map mod 2π in Fig. 5 (centre) reveals several areas of irregular boundaries that have undergone separate motion as indicated by the varying fringe densities and orientations. For spatial unwrapping the areas would need identification and separate evaluation – quite a laborious task. Even more, the saw tooth image

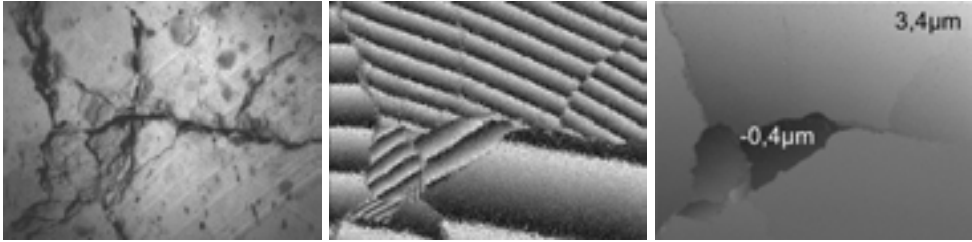


Figure 5. Mapping of out-of-plane displacements in a historic brick specimen due to heat irradiation. Left: white-light image; centre: mod 2π phase map; right: displacement obtained by temporal phase unwrapping.

does not render any information as to the relative heights in the sub-areas because the absolute fringe order within each area is not known – we have no information about the fringe count during the period between capturing images. Yet, this is an important quantity in estimating the distribution of mechanical loads between sub-areas in the specimen.

A solution to this problem is given by temporal phase unwrapping [15]. It makes use of the rapid data rate available in recent image acquisition and processing equipment. The phase history at every single pixel in the camera is stored – in combination with SPS we now get saw tooth data versus time. When images are stored at a rate excluding intermediate phase changes of more than $\pm\pi$ no ambiguous phase jumps are encountered. Thus, we are not bothered by any irregularities in space and unwrapping even yields the relative displacements between the sub-areas. Let us prove this by looking at the result in Fig. 5 right where the amount of displacement is encoded in grey level – ranging from $-0.4\ \mu\text{m}$ at the darkest to $+3.4\ \mu\text{m}$ at the brightest. In such cases, an important question by restorers is whether the deformation in the specimen is reversible and the object follows the cyclic load by cyclic motion. This could, of course, be answered only on the basis of such absolute displacement data as we have obtained them here.

The speed of a process in long-term investigations may differ considerably, e. g., when it is driven by the ambient climate as in many studies on historical objects. In this case, the rate of image storage should be adjusted dynamically. It must be high enough to obey the sampling theorem and as low as possible to save storage space. Once more, temporal phase unwrapping offers a solution, because it provides an instant fringe count. We have used this to trigger the instant of recording images for an optimum number of fringes over the viewing field [16].

Deformation measurements by ESPI rely on the local correlation of the speckle fields scattered from the object surface at different instants of time and are impeded severely when the fields decorrelate. There are two main causes for such effects. The speckle field is altered by the overall motion of the object (geometric decorrelation) or it may change by the minute changes in the surface texture already covered earlier [17]. Either kind of decorrelation will spoil the quality of the measurement and limit the range of applicability.

Often, in-plane motion causes a displacement of the small interrogation areas that are compared in the correlation. A straight-forward calculation with fixed coordinates suffers from a mismatch because only part of the data within each area contributes to correlation. This is especially pronounced in microscopic ESPI where areas of less than a square millimetre are investigated. We had to develop means to cope with this kind of geometric decorrelation. The Fourier-transform technique of handling spatially phase-shifted data provides an elegant way to do so [18].

Recall that the Fourier-transform method re-establishes the complex object-light distribution in the image plane from which we have so far used only the phase data. Yet, we can compute also the intensity distributions that are ordinary speckle images that we would get without the reference wave. Now, we can compare these images by digital image correlation and obtain the in-plane displacement field yielding the mismatch for each interrogation sub-area. The resulting values are used to backshift one of the images for better superposition and then process the ESPI data on optimal matching sub-areas. This method is known as adaptive windowing.

The improvement in the performance thus obtained is best illustrated by examples from microscopic ESPI. In the investigation of stone deterioration, for example, researchers strive to understand how pressure from the crystallization of salts within the porous stone contributes to the weakening of the material. With pore-sizes of typically less than $100\ \mu\text{m}$ deformation measurements request high spatial resolution which can only be obtained under a microscope. For this purpose we have integrated a commercial microscope of long viewing distance into an ESPI setup. Another application is in the study of crack formation in historical paint layers. The famous Chinese terracotta warriors of Lin Tong, for example, loose their invaluable paint cover almost the moment they are excavated, because the originally moist paint layers break up when getting dry. We participate in testing remedies for their conservation.

Fig. 6 was obtained in an ordinary ESPI-study of paint layers on terracotta samples while the humidity was changed – a measuring field of size $230 \times 230\ \mu\text{m}^2$ is inspected. The saw tooth pattern in Fig. 6 (left), obtained in the traditional way, shows useful

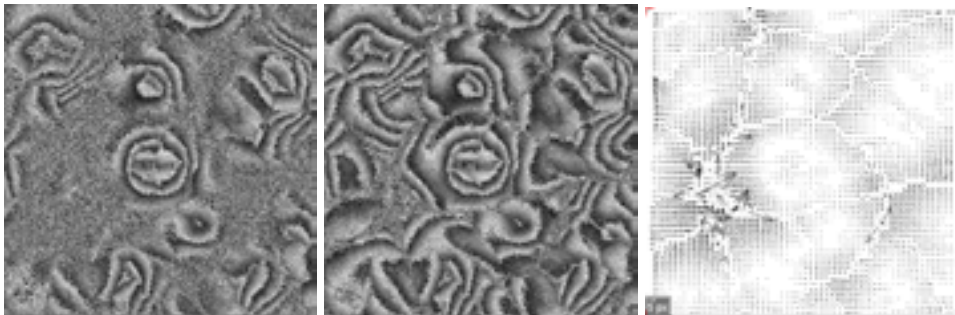


Figure 6. Elimination of geometric decorrelation in microscopic ESPI by adaptive windowing. Object ($230 \times 230\ \mu\text{m}^2$): painted terracotta (Chinese terracotta army) under the influence of humidity. Left: original saw tooth pattern; centre: pattern improved by back-shifted window; right: in-plane deformation vectors.

saw tooth fringes over certain areas, but contains several noisy regions void of fringes because the underlying speckle fields decorrelate. With back-shifting according to the strategy explained above the same data yielded the pattern of Fig. 6 (centre) showing fringes also over most of the area that could not be evaluated before. Obviously, the backshift data also give the in-plane displacement values – indicated by small arrows – supplementing the out-of-plane data from ESPI (Fig. 6, right). It is clearly seen how patches in the image that each can be attributed to a flake of paint move individually. A few spurious displacement vectors are measurement errors and would be eliminated by post-processing. Thus, a single ESPI record can now provide the complete 3D displacement field – a task that usually needs three optical configurations of complementing sensitivity vectors. In case of little surface decorrelation the in-plane component can be obtained with accuracy similar to the out-of-plane component [18].

5 Explorations into the depth: low-coherence speckle interferometry

The optical tools introduced so far make use of light that has been scattered by the specimen and carries mainly information about the location and micro-topography of the surface of a sample. Any conclusions about what is happening in the bulk of the object are indirect. Yet, many practical problems grow underneath the surface of an object and it would be of advantage to have direct access to these regions. As a typical example, take the detachment of paint and varnish layers in the Chinese terracotta-army warriors already mentioned. It is assumed that this stratified heterogeneous compound structure suffers damage because the various layers differ in their mechanical response to the change in ambient humidity. When excavated from the humid soil and moved into dry air, for example, a paint layer may shrink differently from a primary coating or the carrier material. To test such assumptions and provide for countermeasures by conservation agents it would be ideal to map deformations also for various depths in the material.

Light can be used for this purpose if it penetrates deep enough into the material and is sufficiently scattered backwards for detection. When thin paint or varnish layers are involved these are typically only some $100\ \mu\text{m}$ or less in thickness. Often, there is a sufficient amount of light returning from these depths – especially from interfaces – that can be used for metrological purposes. However, a method is needed to discriminate the light according to the depth where it has been scattered. This challenge can be met by making proper use of the coherence of light as in optical coherence tomography (OCT). We have proposed a combination of OCT with ESPI that we call low-coherence speckle interferometry LCSPI [19].

The basic strategy is easily explained. In ESPI, object and reference wave that are obtained by beam-splitting must superimpose coherently to preserve phase information in the CCD-images. Interference of light, however, is only possible when the optical paths travelled by the waves do not differ by more than the coherence length. Usually, researchers avoid worrying about this requirement by using laser-light sources with a coherence length exceeding all scales involved. On the other hand, low-coherence light – as from a super luminescence diode (SLD) of some $50\ \mu\text{m}$

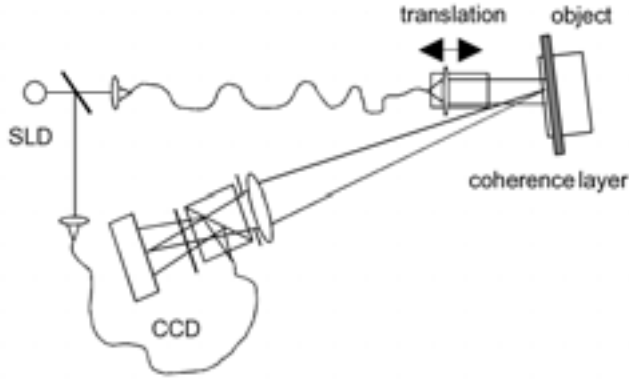


Figure 7. Optical setup for low-coherence speckle interferometry LCSI.

in coherence length – imposes restrictions on interference experiments. With this light source in combination with a proper design of the optics interference patterns can arise only for signals that differ in path accordingly little and thus identify light from a well defined layer in depth.

Fig. 7 explains the optical setup for LCSI. Light from the SLD is coupled into fibres for reference beam and object illumination. While the reference beam is fed into the ESPI optics as usual, the object light exiting from the fibre is collimated by a lens on a translation stage to illuminate the object. The geometric arrangement in the setup defines a thin “coherence layer” in space such that only light scattered within this region contributes to the interferograms evaluated for displacement. Adjustment of position and orientation of the object allows placing this layer in the desired position within the object – at an interface between two paint layers, for example. With the translation stage the coherence layer can then be scanned through the sample for investigations at varying depths.

In practice, the useful interference signal has to compete with a large amount of background light. Furthermore, the useful light has to travel in part through a complex scattering medium that even changes between the instants of observation due to the displacements in the object. Let us, for example, adjust the coherence layer onto an interface between paint and terracotta in a fragment of a Chinese warrior. We are interested in any motion of the interface during drying. On its way to and from the interface, however, the light has to pass through the bulk of paint – a path that quite probably will be influenced during drying. This produces uncorrelated changes in the light and reduces the quality of the resulting fringes. Therefore, the technique will find its limits at a certain depth that we are exploring presently.

For an estimate of the depth range available for exploration a model sample has been studied (Fig. 8) [20]. It was prepared from a partly transparent adhesive (index of refraction $n \approx 2$) that is used in bonding aluminium compounds and that was coated in steps of varying thickness onto a glass plate. The coherence layer was adjusted to the interface between adhesive and glass to observe its out-of-plane motion due to a slight tilt of the specimen. Thus, we observe evenly spaced saw tooth fringes

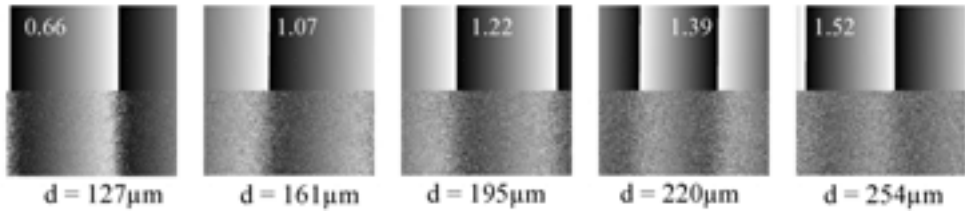


Figure 8. Performance of LCSl through scattering layers of adhesive of different thickness d . Tilt-induced saw tooth fringes for out-of-plane motion of the interface between a glass carrier and the adhesive layer. Lower row: experimental saw tooth fringes; upper row: theoretical fit yielding standard deviations given in rad.

that are parallel to the tilt axis and represent the displacement introduced. With increasing thickness of the layer of adhesive from $127\ \mu\text{m}$ (Fig. 8, left) to $254\ \mu\text{m}$ (Fig. 8, right) the quality of the fringes decreases due to decorrelation of the underlying speckle signals. By fitting ideal fringe functions (shown above each result) to the experimental data the standard deviation σ of the phase in radians is calculated as a measure for fringe quality [11]. The increasing values for σ as given in each fringe set indicate the evident loss in fringe quality with increasing thickness – the maximum possible value is $\sigma = 1.8\ \text{rad}$ and occurs in a random noise pattern that would arise with complete decorrelation. According to our results one can expect to perform successful measurements for a layer thickness of up to a few $100\ \mu\text{m}$ – subject to the specific properties of the material involved.

Let us illustrate the potential of LCSl in an application during out-of-plane measurements on paint layers of the Chinese warriors. Humidity effects were studied in a terracotta fragment that carried a layer of varnish on top of a layer of paint. Thus, in addition to the interface air/varnish at the surface a second reflecting interface was located about $100\ \mu\text{m}$ below the surface. By tuning the coherence layer onto either of these interfaces we wanted to measure relative motions between these layers. Fig. 9 shows deformation fringes in the $1 \times 1\ \text{mm}^2$ sample when the system is tuned to the surface (left) or to the interface (right). The figures give the response to a decrease in ambient relative humidity from 90% to 80%.

The results from the surface indicate clearly that the sample is divided into many small sub-areas that each react by a bowl-shaped deformation due to length changes in the layers. The data originating from the interface at depth $100\ \mu\text{m}$ are more difficult to read as they are noisier – a consequence of the passage of the light through the covering layer. Yet, we see the same separation into bowls, much smaller in deformation, however. A series of deformation maps allows obtaining mean displacement values for both the layers versus measuring time during a cyclic change of the humidity (Fig. 10). We verify the larger response at the top layer – which, of course, includes also the displacement at the lower layer – and realize that there is practically no delay between the reactions of the interfaces. This might be explained by unimpeded passage of humidity through a network of minute cracks separating the bowls.

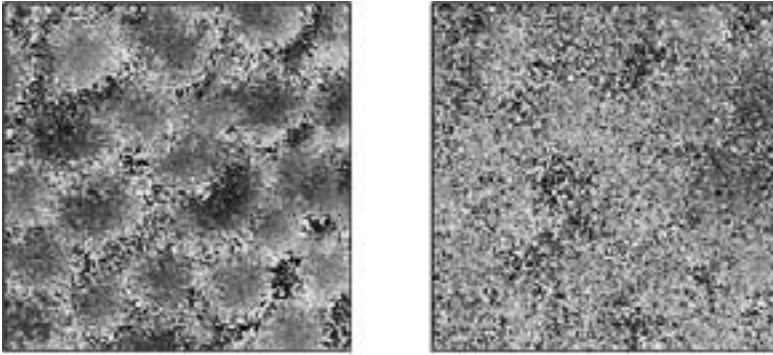


Figure 9. Humidity-induced out-of-plane motion as indicated by saw tooth fringes of the surface (left) and an inner interface at depth 100 μm (right) in a layered coating on a Chinese terracotta sample. Relative humidity changed from 90% to 80%.

In summary, LCSi is a promising tool to explore the deformation scene also within a thin region below the surface of rigid objects. The depth available depends on the optical properties of the material – mostly it will not exceed a millimetre. Since action from an aggressive environment, however, has to penetrate layers immediately adjacent to the surface their mechanical properties become especially important in estimating possible damage.

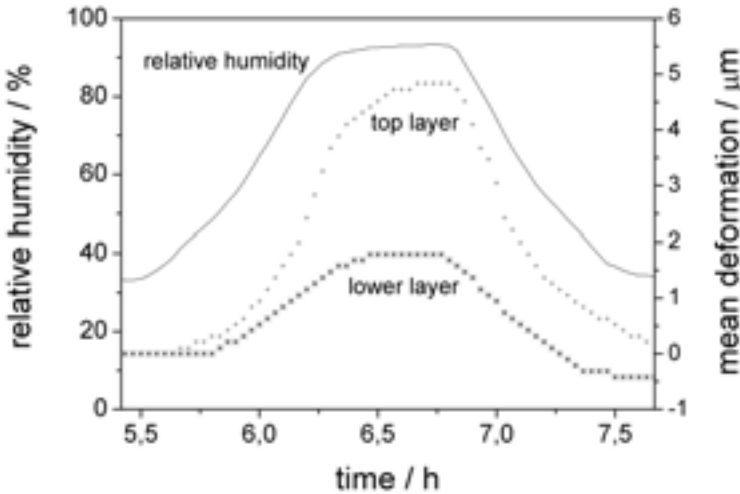


Figure 10. Mean deformation of surface (top layer) and interface (lower layer) in the layered coating on the Chinese terracotta sample of Fig. 8 during the cycle of relative humidity also shown.

6 Sounding the depth by vibration ESPI

Many historical murals are painted on plaster layers of up to several centimetres in thickness. In the course of time, such layers may detach from the supporting wall – thus a check of the integrity of the interface is needed. Conservators usually inspect the condition of wall paintings using the so-called percussion technique, which involves gently tapping the painting, section by section, and deducing from the acoustic response where the plaster is loose. At such locations it sounds “hollow”. Using this method of inspection to plan the restoration of a large church is a cumbersome task requiring complex scaffolding and involving a detailed mapping of the paintings condition that can take months to complete. The obvious solution here would be to develop a measuring technique that can be used to perform this inspection quickly and automatically from ground level, allowing the experts more time to concentrate on the affected areas and their restoration.

We have shown that low-coherence exploration of an object below its surface is possible, but restricted to not much more than a millimetre in depth. Thus, in the present case light can not be used directly to scan the depth for detachments and we must develop other means. We can use the light, however, to probe the minute response of loose areas to an acoustic-wave stimulus coming from a loudspeaker and “sounding” the depth for an optical alert signal.

ESPI is a perfect tool for studying small vibrations [21] that we adapted to the mural problem [22]. In our setup (Fig. 11) an ordinary time average ESPI arrangement is refined by modulation of the reference-beam phase with a frequency slightly displaced from the loudspeaker signal. This has several advantages. In time-average interferometry the fringe function, i. e., the fringe brightness versus vibration amplitude, follows the square of a zero-order Bessel function. As the slope of this function tends to zero for zero amplitude the performance of the method is poor for small vibrations. Reference beam modulation acts as bias amplitude and allows moving the operating point in the fringe function to the place of maximum sensitivity. Furthermore, the beat between reference and signal waves produces flickering light intensities at those

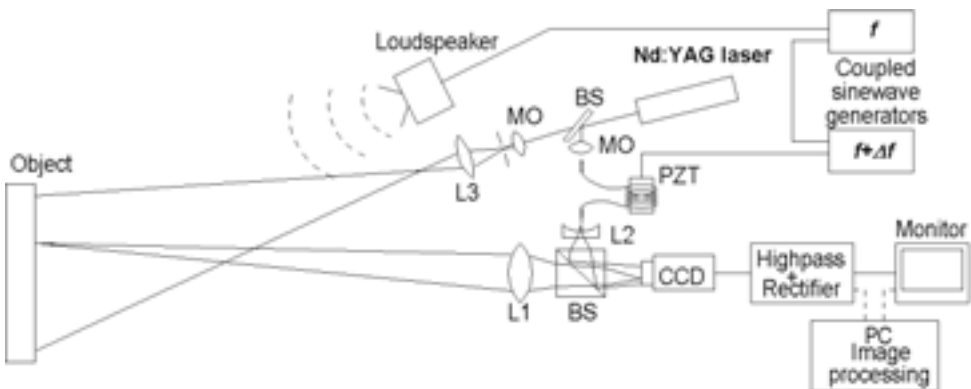


Figure 11. Time average ESPI-system for the study of detached layers in murals.

locations that take part in the vibration. This is a very intriguing feature because it implies intuitively the state of “motion” – a feature important when advertising to the community of restorers and conservators our high-tech method with difficult to read results. Finally, several images captured during a beat cycle provide the basis for temporal phase shifting to yield automated evaluation of vibration amplitude and phase. The final equipment in Fig. 11 is characterized by a fibre-optic reference link which provides the basis for phase modulation (modulation of fibre length by a PZT-driven cylinder) and, if required, allows path length matching by introducing additional fibre. The coherence constraints, however, are low since we changed from our early laser-diode illumination to a very stable CW Nd:YAG laser of many metres in coherence length. Performance is improved by robust setups and averaging over several images which allow doing on-the-site measurements of vibration amplitudes of as little as a few nanometres.

The measurement strategy in mural investigations is to look for resonances while tuning the excitation through an appropriate frequency band. For Fig. 12 the technique was tested at a specially prepared plaster layer on a stone wall that contained an artificially produced region of detachment. This was created by interrupting the mechanical contact between wall and plaster with a plastic foil. We show an amplitude map (left) and a phase map (centre) of a 230-Hz resonance mode in the loose plaster layer. Many such results obtained at 10-Hz frequency steps from 90 Hz to 580 Hz were finally accumulated to produce the final evaluation in the right of Fig. 12. The grey level indicates how often a certain location had responded to the excitation – dark areas vibrated frequently, bright ones rarely; an ordinary object image is put in the background. The location and shape of the loose region are nicely reproduced.

The new technique was put to test on frescos in a cemetery chapel at Kamenz, Saxony. The adhesion of the layers of plaster covering the walls and ceiling was examined one square metre at a time. The frequency of the sound was adjusted in steps of ten Hertz, and the reaction of the wall to each sound was recorded. For the evaluation it was again calculated how often an oscillation was detected for each position on the wall. This time the data obtained was assigned colour values, so



Figure 12. ESPI-study of vibrations of an artificially produced detachment in a plaster layer on a stone wall. Left: amplitude map of 230-Hz higher-order mode of the plaster plate; centre: corresponding phase map; right: final evaluation of excitation response between 90 Hz and 580 Hz in 10 Hz-steps indicating the loose area (dark illustrates frequently, bright rarely excited regions) – an ordinary object image in the background.

that all of the areas where there was no longer good adhesion to the substrate were eventually displayed in yellow or red. Here, the new laser-optical technique passed successfully when its results were compared to those obtained using the conventional percussion method. It benefited from the advantage that the damaged areas shown on the video image could be located precisely and automatically. Manual mapping performed by a conservator, on the other hand, can easily contain errors that creep in during the mapping process.

A famous example of where our method has been applied is the church of the Benedictine Convent of Saint John at Müstair in Graubünden, Switzerland, which has been declared a UNESCO World Heritage Site because of its medieval wall paintings. In the 12th century, the original Carolingian frescos, which had been painted 300 years before, were covered by a new layer of plaster and a series of Romanesque wall paintings. To roughen the surface in preparation for the new plaster, in parts even holes were pounded in the Carolingian paintings. Nevertheless, the adhesion between the older and the more recent plaster is poor in many places, which has caused parts of the newer paintings falling off the wall. Using the laser-optical measuring technique, it has been possible to identify large loose sections in many places, which can now be kept under close observation by conservators. This is demonstrated in Fig. 13 that shows the colour-coded result obtained from a wall in the south apse of the church. Again, loose sections are those areas that vibrated often and thus are indicated by red or yellow, the intact portions that could hardly be excited are coloured green to blue. Contours of the paintings are overlaid to indicate the location in the mural. At some points, it may be necessary to reinforce the connection between plaster and substrate. One alarm signal would be if these damaged sections were to become larger – possibly as a consequence of a minor earthquake that shook Graubünden in 2001. This will now be confirmed by comparing the earlier data with data from a repeat measurement. Here, an advantage over the traditional method of manual testing is its objectiveness which is important in such a comparison.

Additional information from the vibration data can be utilized for more detailed depth sounding. Thick layers respond at low, thin layers at higher frequencies. In a multi-layer plaster this allows speculations about the depth of the damaged interface. For an example, we present results of a study on a two-layer plaster coating at a historical wall of the Neues Museum, Berlin that was checked for the success of a remedy in which restorers had injected fixing cement through a certain number of small holes. Preliminary studies at a location where the upper layer was missing revealed that the lower layer responded mostly to frequencies below some 800 Hz. Thus, we grouped our results into two maps, one considering all data below, the other those above 800 Hz. In Fig. 14, hatching from upper left to lower right indicates regions where the lower interface (response to frequencies below 800 Hz) is considered loose; hatching from lower left to upper right indicates according regions for the upper interface (frequencies above 800 Hz). The width of the scene was 0.9 m; the bright dots give locations of cement injections. The results clearly show that the lower interface was not repaired as we find one large vibrating region in the low-frequency domain that includes the location of many of the fixation points. The response of the thinner upper layer (indicated by the many small regions in the high-frequency map) respects most of these points. Probably, the holes did not penetrate through

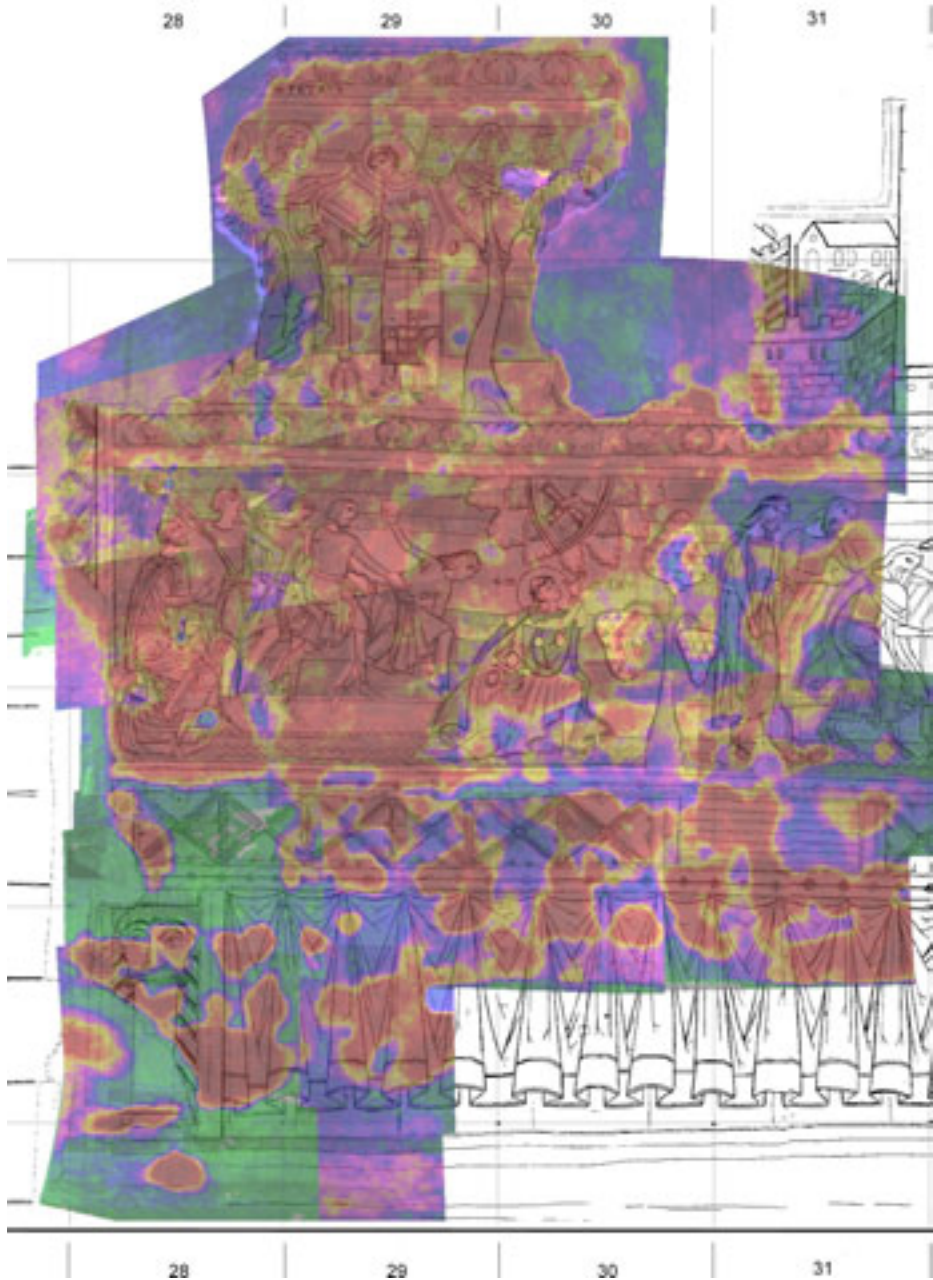


Figure 13. Map of loose areas in a Romanesque fresco of the south apse in St. John's Church of the World Heritage Site Müstair in Graubünden, Switzerland. Vibration ESPI results indicate intact regions by green/blue, loose areas by red/yellow. Height of the scene some 5 metres; the drawing describes the historical painting.

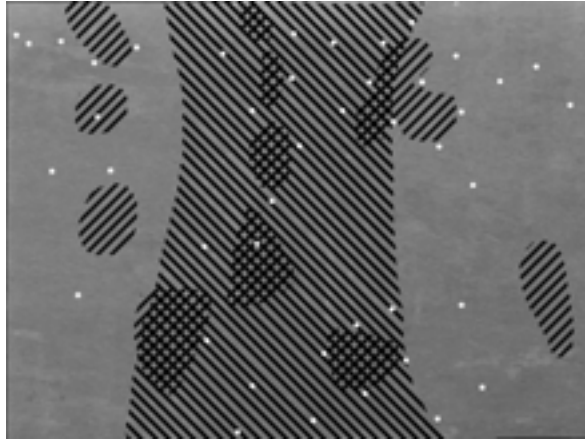


Figure 14. Localization of detachments in a two-layer plaster on a wall in Neues Museum, Berlin. Results of a series of ESPI measurements at equidistant frequencies. Hatching from upper left to lower right indicates regions where the lower interface (response to frequencies below 800 Hz) is considered loose; hatching from lower left to upper right indicates according regions for the upper interface (frequencies above 800 Hz). The bright dots give locations of cement injections.

the second layer and the cement connected only the two layers, but did not attach them to the wall.

7 Conclusions

Techniques of coherent optical metrology have proven well-suited for the investigation of the mechanical processes involved in the deterioration of artwork. They offer the necessary sensitivity to explore displacement fields and surface changes, and they are non-invasive which is of essential importance in delicate historical pieces. While the basic usefulness has been shown in various problems the metrology must now be developed for general acceptance as a tool in the everyday tasks of restorers and conservators.

Acknowledgements

This account is a summary of work that has been carried out mainly in the Applied Optics Group at the Institute of Physics in Oldenburg. The dedicated contributions of many members of the group throughout the years enter into the result which is acknowledged gratefully. Since the very beginning G. Gülker and H. Helmers have been involved in many of the studies. Special mention deserves the doctoral thesis work of J. Burke, T. Fricke-Begemann and H. Joost, who have contributed essentially to our progress in speckle metrology. Recent advances in LCSi are benefiting from cooperation with K. Gastinger at SINTEF, Trondheim, Norway. We also acknowledge the financial support from DFG, BMBF and DBU.

References

- [1] D. Paoletti and G. S. Spagnolo, 'Interferometric methods for artwork diagnostics', in *Progress in Optics* (Elsevier, 1996), vol. XXXV, pp. 197–255.
- [2] K. Hinsch and G. Gülker, 'Lasers in art conservation', *Physics World* **14**, 37 (2001).
- [3] G. Gülker, H. Helmers, K. D. Hinsch, P. Meinschmidt, and K. Wolff, 'Deformation mapping and surface inspection of historical monuments', *Opt. Las. Eng.* **24**, 183 (1996).
- [4] H. J. Dainty, *Laser Speckle and Related Phenomena* (Springer, Berlin, 1975).
- [5] M. Sjödaahl, 'Digital speckle photography', in *Digital Speckle Pattern Interferometry and Related Techniques*, edited by P. K. Rastogi (Wiley, Chichester, 2001).
- [6] K. D. Hinsch, G. Gülker, H. Hinrichs, and H. Joost, 'Artwork monitoring by digital image correlation', in *Lasers in the Conservation of Artworks*, edited by K. Dickmann, C. Fotakis, and J. F. Asmus (Springer, Berlin, 2004), LACONA V Proceedings.
- [7] T. Fricke-Begemann, 'Three-dimensional deformation field measurement with digital speckle correlation', *Appl. Opt.* **42**, 6783 (2003).
- [8] T. Fricke-Begemann and K. D. Hinsch, 'Measurement of random processes at rough surfaces with digital speckle correlation', *J. Opt. Soc. Am. A* **21**, 252 (2004).
- [9] R. Jones and C. Wykes, *Holographic and Speckle Interferometry* (Cambridge University Press, Cambridge, 1983).
- [10] K. Creath, 'Phase-shifting speckle interferometry', *Appl. Opt.* **24**, 3053 (1985).
- [11] J. Burke, *Application and optimization of the spatial phase shifting technique in digital speckle interferometry*, Dissertation, University of Oldenburg (2000).
- [12] T. Bothe, J. Burke, and H. Helmers, 'Spatial phase shifting in electronic speckle pattern interferometry: minimization of phase reconstruction errors', *Appl. Opt.* **35**, 5310 (1997).
- [13] M. Takeda, H. Ina, and S. Kobayashi, 'Fourier-transform method of fringe-pattern analysis for computer-based topography and interferometry', *J. Opt. Soc. Am.* **72**, 156 (1982).
- [14] J. Burke, H. Helmers, C. Kunze, and V. Wilkens, 'Speckle intensity and phase gradients: influence on fringe quality in spatial phase shifting ESPI-systems.', *Optics Comm.* **152**, 144 (1998).
- [15] J. Huntley and H. Saldner, 'Temporal phase-unwrapping algorithm for automated interferogram analysis', *Appl. Opt.* **32**, 3047 (1993).
- [16] J. Burke and H. Helmers, 'Matched data storage in ESPI by combination of spatial phase shifting with temporal phase unwrapping', *Opt. Las. Technol.* **32**, 235 (2000).
- [17] G. Gülker and K. D. Hinsch, 'Detection of surface microstructure changes by electronic speckle pattern interferometry', *J. Opt. Las. Eng.* **26**, 165 (1997).
- [18] T. Fricke-Begemann and J. Burke, 'Speckle interferometry: three-dimensional deformation field measurement with a single interferogram', *Appl. Opt.* **40**, 5011 (2001).
- [19] G. Gülker, K. D. Hinsch, and A. Kraft, 'Deformation monitoring on ancient terracotta warriors by microscopic TV-holography', *Opt. Las. Eng.* **36**, 501 (2001).
- [20] K. Gastinger, G. Gülker, K. D. Hinsch, H. M. Pedersen, T. Stren, and S. Winther, 'Low coherence speckle interferometry (LCSI) for detection of interfacial instabilities in adhesive bonded joints', in *Proc. SPIE vol. 5532* (SPIE, Bellingham, 2004), p. 256.
- [21] S. Ellingsrud and G. O. Rosvold, 'Analysis of a data-based TV-holography system used to measure small vibration amplitudes', *J. Opt. Soc. Am. A* **9**, 237 (1992).
- [22] G. Gülker, K. D. Hinsch, and H. Joost, 'Large-scale investigation of plaster detachments in historical murals by acoustic stimulation and video-holographic detection', in *Proc. SPIE vol. 4402* (SPIE, Bellingham, 2001), p. 184.